JOURNAL OF MATERIALS SCIENCE 28 (1993) 4245–4249

A microtexture study of eutectic carbides in white cast irons using electron back-scatter diffraction

V. RANDLE
University College, Swansea SA2 8PP, UK
G. LAIRD II
US Bureau of Mines, Albany Research Center, Albany, OR 97321, USA

White cast irons have a microstructure composed of a ferrous matrix with hexagonal and/or orthorhombic carbides, M_7C_3 and M_3C, respectively. The US Bureau of Mines has implemented a study programme to improve microstructure and thereby wear resistance of these alloys. This work included electron back-scatter diffraction in a scanning electron microscope to identify the hexagonal and orthorhombic phases from their crystallography and subsequently establish their microtextures. Crystal structures of these carbides were identified and their microtextures were obtained from specific spatial locations within micrometre resolution. Such resolution allowed the identification of thin shells of M_3C (1–5 μm thick) to be distinguished from cores of M_7C_3 (10–20 μm thick). Microtexture results showed that M_7C_3 carbides without M_3C shells grew predominantly in the [0 0 0 1] direction, whereas those with M_3C shells were much less textured with the M_3C shell phase having a random microtexture.

1. Introduction

White cast irons are widely used in environments where high abrasion and impact resistance is of major importance. Essentially their microstructure consists of hexagonal and/or orthorhombic carbides embedded within a face-centred cubic austenitic (γFe) and/or body-centred tetragonal martensitic matrix [1–3]. The US Bureau of Mines has implemented a study programme to improve the wear-resistant properties of these alloys by exploiting certain aspects of their carbide morphology and phase structure [4–6]. In this report, a feasibility assessment is given of applying electron back-scatter diffraction (EBSD) to both identification of the constituent phases and subsequent microtexture measurement in these irons.

EBSD is a relatively new scanning electron microscope (SEM)-based technique which allows orientations (textures) to be measured on an individual, spatially specific basis from phases identified by the crystallographic information contained in the diffraction pattern [7–9]. EBSD is, in most cases, the optimum means of obtaining "microtexture" (i.e. spatially specific orientations) and has been applied extensively to cubic materials which can be readily analysed on-line within the SEM (e.g. [10–13]). The particular attraction of EBSD for microstructural studies of white cast irons is that investigations are carried out on bulk polished specimens. Alternatively, if transmission electron microscopy is used the disparate nature of the iron specimen renders foil preparation a difficult task.

Hitherto, the application of EBSD to the microtexture of crystal structures which are more complex than cubic has not been explored in detail. Primarily, the interpretation of the Kikuchi diffraction pattern becomes increasingly difficult as the crystal symmetry decreases. Once diffraction patterns are unambiguously identified and indexed for a whole stereographic unit triangle of the particular crystal system, microtexture measurement becomes a pattern-matching routine. The data reported here illustrate these procedures for both the hexagonal and orthorhombic carbide phases. The ultimate aim of measuring the orientations and orientation relationships between phases in these white cast irons is to elucidate the growth mechanisms of the constituent carbides.

2. Experimental procedure

Two types of white cast iron specimens were examined and their compositions are given in Table I. Both specimens were sectioned from the interiors of larger 200 g samples that were slow cooled at 0.017 $K\,s^{-1}$ from the liquidus. Fig. 1a and b show scanning electron micrographs of Specimens 1 and 2 after deep etching with 75% HCl, 24% HNO_3 and 1% HF (all wt %) to remove the ferrous matrix. The view shown in Fig. 1a is of an eutectic colony in Specimen 1 consisting entirely of hexagonal metal carbides having a stoichiometry of M_7C_3 [1, 2]. Fig. 1b shows the duplex carbide morphology of Specimen 2. These

0022–2461

TABLE I Compositions of Specimens 1 and 2. Heavy elements were measured by X-ray fluorescence and carbon by gas analysis.

Specimen	Composition (wt %)					
	Fe	Cr	Ni	C	Si	Total (%)
1	81.6	8.9	6.2	3.26	2.3	102.4
2	82.6	8.6	5.7	3.69	0.3	100.9

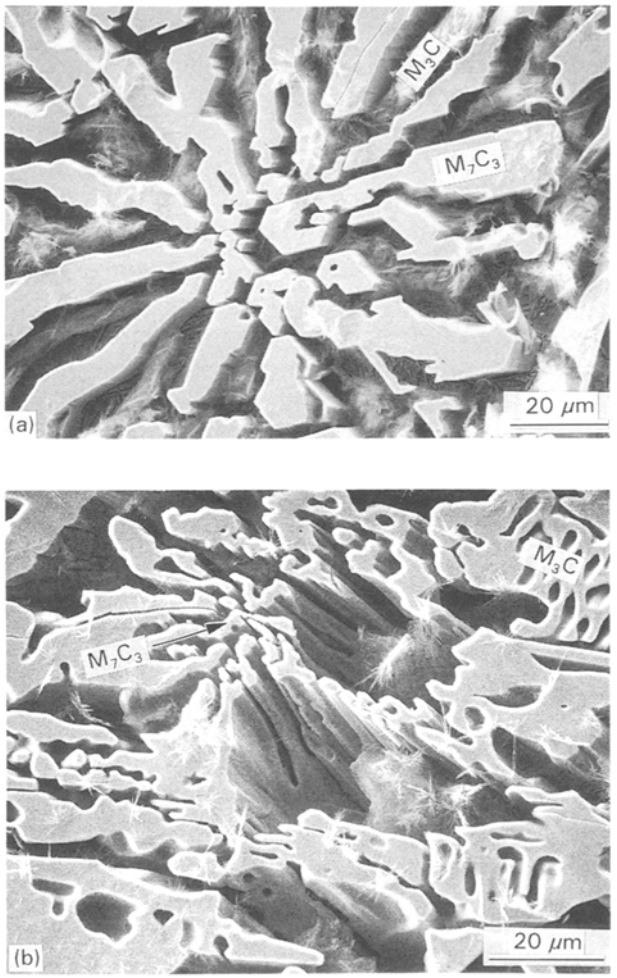

Figure 1 Scanning electron micrographs of deep-etched Specimens 1 (a) and 2 (b). Specimen 1 consists entirely of hexagonal M_7C_3 eutectic carbide while Specimen 2 consists of a duplex mixture of hexagonal M_7C_3 and orthorhombic M_3C carbide. The clusters of small needles appearing in both (a) and (b) are M_3C carbides formed by solid-state reaction upon cooling (marked in a).

carbides consist of thin shells (1–5 μm) of orthorhombic carbide with a stoichiometry of M_3C surrounding cores (10–20 μm) of hexagonal M_7C_3 carbide [1, 2]. In this latter specimen, duplexing results from an initial eutectic reaction of $L \rightarrow M_7C_3 + \gamma Fe$ followed by a peritectic reaction of $L + M_7C_3 \rightarrow M_3C + \gamma Fe$. The carbide morphology of Specimen 2 consists of rods, laths, and some plate-like forms which are attributed to the orthorhombic M_3C carbide.

One method of discriminating between the M_3C shells and M_7C_3 cores is to use the electron backscatter mode in the SEM [1]. Fig. 2 shows the various phases that can be identified in Specimen 2 via atomic number differences under such imaging. This feature

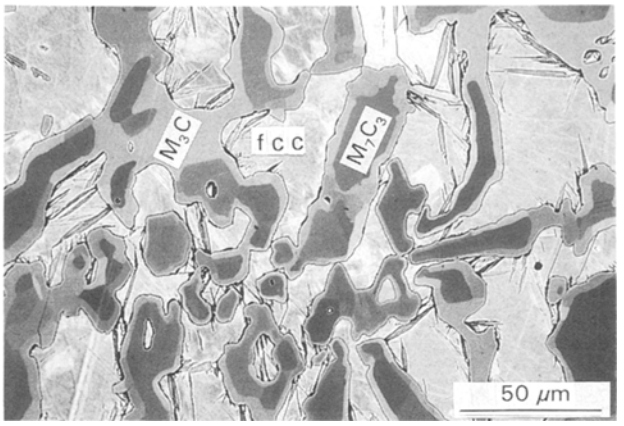

Figure 2 Electron backscatter micrograph of Specimen 2. The cores of low-density hexagonal M_7C_3 carbides appear dark next to the shells of higher density orthorhombic M_3C carbides. The fcc austenite appears the lightest with some plates of martensite appearing as dark streaks within the austenite.

allowed a simple verification of on-line EBSD observations. It should be noted that additional details of the chemistry and formation of these irons can be found elsewhere [1, 2].

The hexagonal M_7C_3 is classified as point group $6/mmm$ (holosymmetric) which has a rotation hexad and perpendicular mirror plane associated with the [0001] axis combined with a diad and mirror plane associated both with the x, y, u axes and with the directions $\langle 11\bar{2}0 \rangle$ [14]. The lattice parameters are $a = 0.6921$ nm and $c = 0.4508$ nm [2]. The orthorhombic M_3C is point group mmm (holosymmetric) which has a rotation diad and a mirror plane associated with each of the reference axes x, y, z [14] with lattice parameters of $a = 0.5070$, $b = 0.6733$, and $c = 0.4520$ nm [2].

After metallographic preparation, specimens were polished in a Syton silica/alkali suspension to remove any surface damage which might otherwise degrade the quality of the diffraction patterns. EBSD work was performed in a Jeol 840 SEM using a probe voltage of 20 kV and a current of 10 nA.

Diffraction patterns were simultaneously viewed on a monitor screen and recorded on photographic film using a plate camera. The camera was assembled and built in-house at Bristol University. The photographic image offers two distinct advantages over interrogating the live pattern; more detail is resolved within the Kikuchi pattern and the angular field of view is greater, typically $85° \times 60°$.

3. Discussion

3.1. Diffraction patterns

Materials having cubic symmetry allow the ready identification of major poles from their diffraction patterns: this is the basis of on-line orientation determination. In the present work, diffraction patterns from the carbides could not be readily indexed on-screen: in fact, it was usually impossible to differentiate between hexagonal and orthorhombic patterns. An exception was the case when the hexad axis, which is

easy to recognize because of its striking six-fold symmetry, was near the centre of the pattern. Otherwise orientations were often obtained from photographically recorded patterns.

An essential part of the pattern recognition and interpretation process was the formulation of hexagonal and orthorhombic Kikuchi maps covering a complete stereographic unit triangle. The area of the hexagonal and orthorhombic triangles were 1/24 and 1/8 of the respective reference spheres. Identification of individual patterns was performed by identifying the crystal symmetry elements (i.e. mirror planes, rotation axes) in concert with the measurement of the interzonal or interplanar angles. This latter measurement was simplified through the use of an EBSD pattern simulation program [15]. Lastly, for both visual inspection and angular measurements the distortions inherent in gnomonic projection had to be taken into account.

Fig. 3 shows the indexed Kikuchi map for the hexagonal phase. The three mirror planes and corresponding major zone axes are labelled. Patterns may either match directly or be mirror reflected with respect to the map, which means that the indexing must be adjusted accordingly to allow for the handedness of the hexagonal unit triangle.

Fig. 4 is the Kikuchi map for the orthorhombic phase. Although only two diffraction patterns were required for the hexagonal Kikuchi map, the orthorhombic map required several patterns. In the former, the spherical triangle has an angular area of $90° \times 90° \times 30°$ whilst the latter encompasses a much larger area of $90° \times 90° \times 90°$. A further consequence of the large angular area in the orthorhombic case is that its sphericity precludes straightforward representation of the whole map in two dimensions, that is, on the printed page. Hence, Fig. 4 is presented in two parts which join at a and b as labelled. The crystal axes [0 0 1], [0 1 0] and [1 0 0] are labelled. Orientations from orthorhombic carbides are obtained by reference to the unit triangle map in a similar manner to that for hexagonal carbides. In both cases, the hexagonal and orthorhombic Kikuchi maps provide all the necessary information to index subsequent patterns for both carbides.

3.2. Microtexture measurements

Fig. 5a and b are inverse pole figures of the direction normal to the specimen surface for hexagonal M_7C_3 carbides in Specimens 1 and 2, respectively. For convenience all data were plotted in a single unit triangle. Microtexture analysis of Specimen 1 reported in Fig. 5a, containing only eutectic hexagonal M_7C_3 carbides was confined to one eutectic colony. Furthermore, this colony was selected such that the sectioned plane appeared to intersect the carbides dominant growth direction, i.e. the [0 0 0 1] axis. Hence, the purpose of this microtexture assessment was to determine whether or not individual carbides within the eutectic colony grow under coupled conditions. Fig. 5a shows that a very strong microtexture exists along the [0 0 0 1] axis. This evidence of a preferred growth direction is in accord with transmission electron microscopy studies done by Pearce [16]. In addition to the quantitative data in Fig. 5a, many other qualitative observations on other eutectic colonies similarly oriented were made supporting this very strong microtexture and hence coupled growth within individual eutectic colonies. Although coupled growth during unidirectional solidification of Fe–Cr–C alloys is well known [17–19], the nucleation and growth behaviour of randomly oriented eutectic grains in these alloys is not well known. This very interesting result of coupled growth within the Fe–Cr–C eutectic grain supports the hypothesis by Powell [20] that growth occurs from a single nucleation site. Therefore, if the number of heterogeneous nucleation sites could be increased,

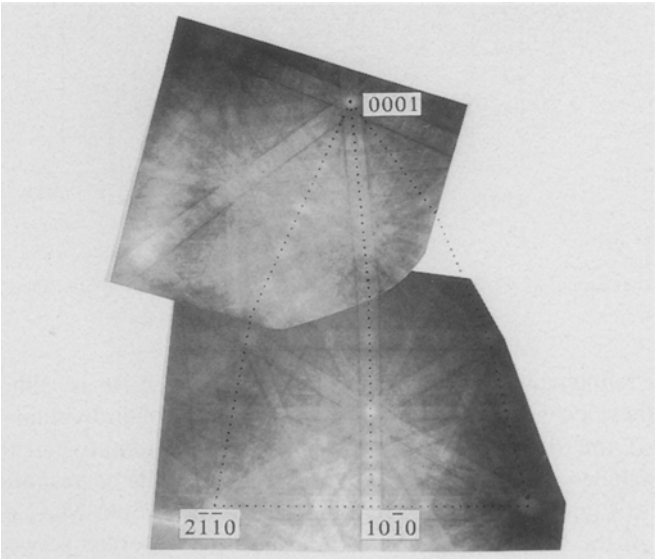

Figure 3 Kikuchi map for hexagonal M_7C_3 carbide showing the 1/24 unit triangle that is sufficient for all subsequent hexagonal carbide pattern matching.

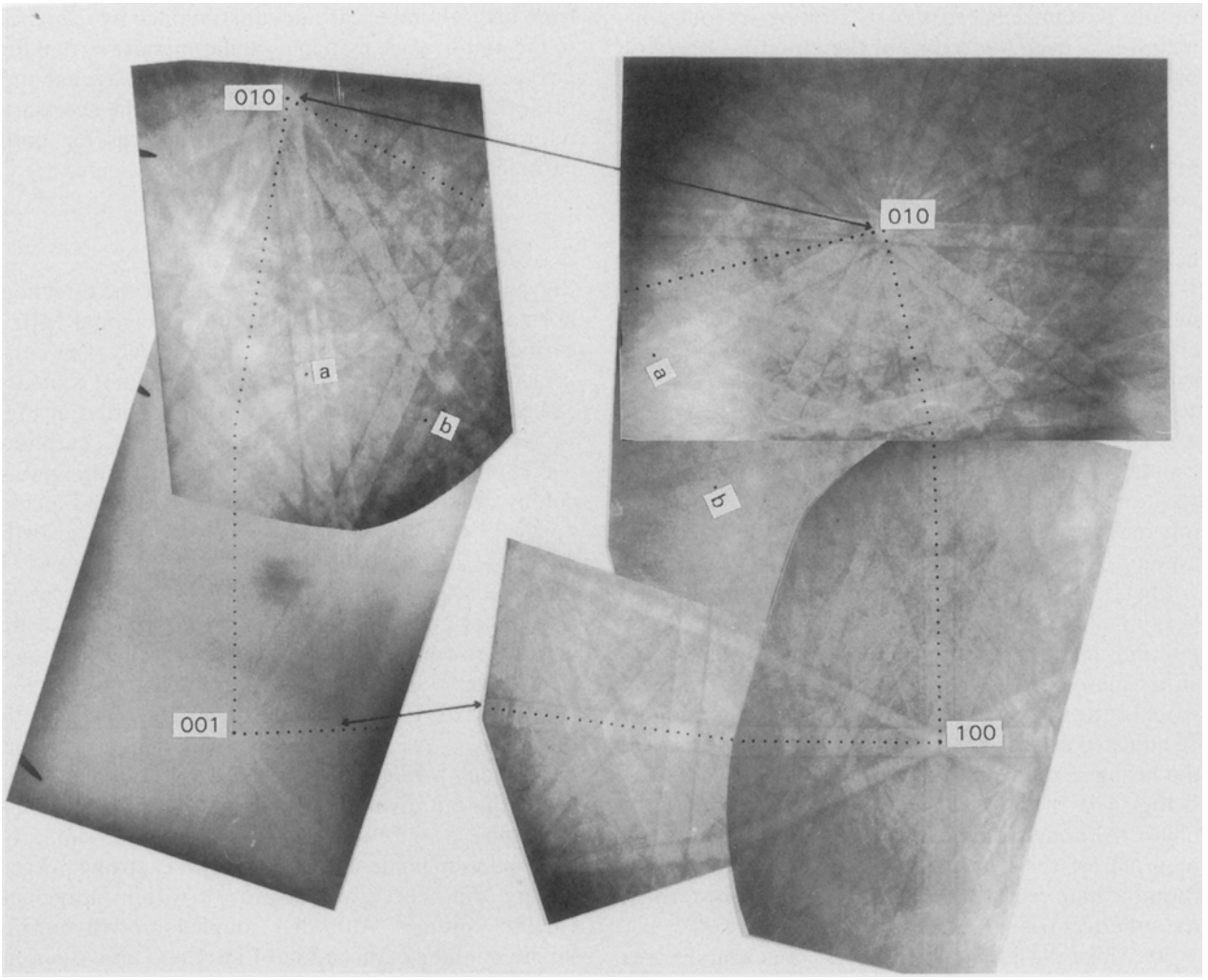

Figure 4 Kikuchi map for orthorhombic M_3C carbide showing the 1/8 unit triangle that is sufficient for all subsequent orthorhombic carbide pattern matching.

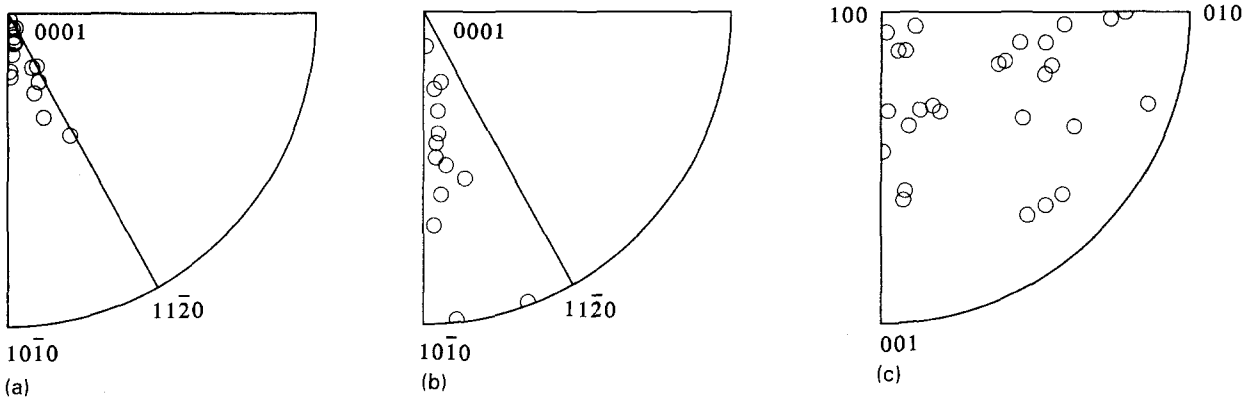

Figure 5 Inverse pole figures of (a) hexagonal M_7C_3 from Specimen 1 (b) hexagonal M_7C_3 from Specimen 2, and (c) orthorhombic M_3C from Specimen 2.

then it would follow that a refinement of the eutectic grain size would occur in these Fe–Cr–C alloys.

However, in Specimen 2 the duplex (hexagonal core/orthorhombic shell) carbides indicate a far more random texture as shown in Fig. 5b. It appears that the growth characteristics of the hexagonal carbides were modified during the peritectic growth of the orthorhombic shell. Owing to the nature of the peritectic reaction of absorbing some of the former hexagonal carbide, it is difficult to measure the exact orientation of individual hexagonal cores. As such, this result is tentative at this time.

Fig. 5c is the corresponding inverse pole figure for the orthorhombic M_3C phase. No orientation relationship is observed between individual orthorhombic carbides. It would appear that although it is likely that the orthorhombic carbide would nucleate on the existing hexagonal carbides, no specific nucleation rela-

tionship dominates the subsequent carbide growth. This result is plausible considering the rapid and orthotropic growth characteristics of the orthorhombic carbide in Fe–C alloys [21, 22].

4. Conclusions

One important feature of this work is that Kikuchi maps are presented for the unit triangles of hexagonal M_7C_3 and orthorhombic M_3C carbides. With these maps it was possible to interrogate numerous hexagonal and orthorhombic carbides for microtexture relationships on a micrometre basis over a large spatial area. This key ability to cover large areas on one contiguous specimen allows definitive microtexture measurements to be made, for the first time, over many Fe–Cr–C eutectic grains.

Application of this technique allowed the following conclusions to be drawn.

1. A strong preferred [0001] growth direction exists for the Fe–Cr–C hexagonal carbide in white cast irons.

2. Coupled growth occurs within the eutectic grain of the Fe–Cr–C specimen containing only hexagonal carbides.

3. Such coupled growth is believed to occur from a single nucleation site within the eutectic grain.

4. No specific microtexture relationship could be discerned for the duplex carbide consisting of a hexagonal core surrounded by an orthorhombic shell.

5. Fe–Cr–C orthorhombic carbides exhibit no sign of coupled growth during peritectic solidification.

Acknowledgements

The authors thank Mr Stephen T. Anderson for photographic assistance, and Dr G. L. F. Powell for his thoughtful critique.

References

1. G. LAIRD II, R. L. NIELSEN and N. H. MACMILLAN, *Metall. Trans.* **22A** (1991) 1709.
2. G. LAIRD II, R. R. BROWN and R. N. NIELSEN, *Mater. Sci. Technol.* **7** (1991) 631.
3. G. L. F. POWELL and G. LAIRD II, *J. Mater. Sci.* **27** (1992) 29.
4. G. LAIRD II, W. K. COLLINS and R. BLICKENSDERFER, *Wear* **124** (1989) 217.
5. R. BLICKENSDERFER, J. H. TYLCZAK and G. LAIRD II, in "Wear of Materials", edited by K. C. Ludema (ASME, New York), p. 175.
6. G. LAIRD II, *Trans. AFS* **96** (1988) p. 799.
7. D. J. DINGLEY, *Scan. Elect. Micros.* **11** (1984) 569.
8. D. J. DINGLEY and V. RANDLE, *J. Mater. Sci.*, in press.
9. V. RANDLE, "Microtexture Determination and its Applications" (Institute of Metals, London, 1993).
10. D. JUUL JENSEN, N. HANSEN and Y. L. LIU, *Mater. Sci. Technol.* **7** (1991) 369.
11. J. HJELEN, R. ORSUND and E. NES, *Acta Metall. Mater.* **39** (1991) 1377.
12. S. I. WRIGHT and B. L. ADAMS, *Textures Microstruct.* **12** (1990) 65.
13. V. RANDLE and A. BROWN, *Philos, Mag.* **59A** (1989) 1075.
14. D. McKIE and C. McKIE, in "Crystalline Solids" (Nelson, London, 1974).
15. K. BABA-KISHI, PhD thesis, University of Bristol (1986).
16. J. T. H. PEARCE, *J. Mater. Sci. Lett.* **2** (1983) 428.
17. E. FRAS, E. GUZIK and H. F. LOPEZ, *Metall. Trans.* **19A** (1988) 1235.
18. Y. MATSUBARA, K. OGI and K. MATSUDA, *Trans. AFS* **89** (1981) 183.
19. K. OGI, Y. MATSUBARA and K. MATSUDA, *ibid.* **89** (1981) 197.
20. G. L. F. POWELL, in Proceedings of the 35th Annual Conference of the Australasian Institute of Metals, Sydney, May 1982, p. 57.
21. R. ELLIOTT, "Cast Iron Technology" (Butterworths, London, 1988) p. 103.
22. M. HILLERT and V. V. SUBBA RAO, in "The Solidification of Metals", Vol. 110 (Iron Steel Institute, London, 1968) p. 204.

Received 3 September 1992
and accepted 11 January 1993